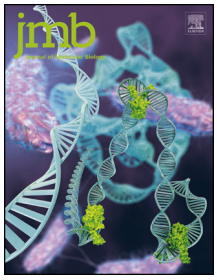

# Structural Basis of Interleukin-5 Inhibition by the Small Cyclic Peptide AF17121

**Jan-Philipp Scheide-Noeth, Maximilian Rosen, David Baumstark, Harald Dietz and Thomas D. Mueller**

***Department of Molecular Plant Physiology and Biophysics,*** *Julius-von-Sachs Institute of the University Wuerzburg, Julius-von-Sachs-Platz 2, D-97082, Wuerzburg, Germany*

***Correspondence to Thomas D. Mueller:*** *mueller@biozentrum.uni-wuerzburg.de*
https://doi.org/10.1016/j.jmb.2018.11.029
***Edited by Sachdev Sidhu***

## Abstract

Interleukin-5 (IL-5) is a T-helper cell of subtype 2 cytokine involved in many aspects of eosinophil life. Eosinophilic granulocytes play a pathogenic role in the progression of atopic diseases, such as allergy, asthma and atopic dermatitis and hypereosinophilic syndromes. Here, eosinophils upon activation degranulate leading to the release of proinflammatory proteins and mediators stored in intracellular vesicles termed granula thereby causing local inflammation, which when persisting leads to tissue damage and organ failure. As a key regulator of eosinophil function, IL-5 therefore presents a major pharmaceutical target and approaches to interfere with IL-5 receptor activation are of great interest. Here we present the structure of the IL-5 inhibiting peptide AF17121 bound to the extracellular domain of the IL-5 receptor IL-5Rα. The small 18mer cyclic peptide snugly fits into the wrench-like cleft of the IL-5 receptor, thereby blocking access of key residues for IL-5 binding. While AF17121 and IL-5 seemingly bind to a similar epitope at IL-5Rα, functional studies show that recognition and binding of both ligands differ. Using the structure data, peptide variants with improved IL-5 inhibition have been generated, which might present valuable starting points for superior peptide-based IL-5 antagonists.



## Introduction

Eosinophils exert important functions in host protection during innate and adaptive immunity. A feature of these leucocytes is vesicular compartments termed granula, which contain toxic and pro-inflammatory substances and proteins. Upon activation, these are released and are key to the defense reaction against extracellular pathogens [1]. While helminths were initially considered the target [2], eosinophils nowadays play a major role in atopic diseases [3]. Whether this is a physiologically desired response or an unwanted dysregulation is still matter of debate [4]. Atopic diseases, for example, allergy, asthma or neurodermatitis, show elevated numbers of eosinophils in the lung, skin and blood, where they cause inflammation accounting for the typical symptoms. Hypereosinophilic syndromes are another, albeit rare form of eosinophilia. They affect a wide range of organs and tissues and will be fatal, if untreated [5]. The usually idiopathic hypereosinophilic syndrome and atopic eosinophilia share a persistent inflammation due to activated eosinophils, which causes fibrosis and damages affected tissues and organs. The central role of eosinophils in the above-described diseases indicates that their removal or inhibition presents a promising strategy to fight eosinophilia.

As interleukin (IL)-5 is a key regulator of eosinophils involved in many aspects of eosinophil life, for example, differentiation, migration, survival and activation, it became a target for pharmaceutical intervention [6,7]. It signals through a heterodimeric cell-surface receptor, which is assembled by a sequential mechanism. Here, IL-5 binds first to IL-5Rα (CD125) and then recruits the so-called common beta chain, βc (CD131) to form a ternary complex [8]. As βc is also utilized by IL-3 and granulocyte–macrophage colony-stimulating factor (GM-CSF) [9,10] direct inhibition of either IL-5 or IL-5Rα seems superior to specifically abrogate IL-5 signaling. Several approaches have been

established employing neutralizing antibodies directed against either IL-5 or IL-5Rα [11,12]. Although some of these antibodies have been approved by FDA/EMA for treatment of severe asthma recently, they share the disadvantage of being large and expensive biologicals, which require administration in high doses. In addition, the antibodies might be targeted by the immune system themselves, when administered long-term, and could therefore lose their efficacy. Another approach to block IL-5 signaling has been reported utilizing small peptides that directly bind to IL-5Rα and competitively block the receptor's interaction with IL-5 [13,14]. Two groups of IL-5 inhibiting peptides were identified: monomeric cyclic peptides and disulfide-bridged homodimeric peptides. While these peptides block IL-5 signaling *in vitro* very effectively, little is known about their mechanism of action [14–17]. Further improvement to make them alternatives to the above-mentioned biologicals in the treatment of eosinophil-mediated diseases, however, would require knowledge about their mechanism of receptor inhibition.

Here we report the first crystal structure of the IL-5 inhibitory peptide AF17121 bound to the IL-5 receptor IL-5Rα. Together with an in-depth structure–function analysis, we could unravel the mechanism by which the peptide is recognized by IL-5Rα and blocks interaction of IL-5Rα with IL-5. These data will facilitate rational design of improved IL-5 inhibiting peptides or small-molecule-based pharmacophores yielding novel therapeutics against atopic diseases or the hypereosinophilic syndrome.

**Table 1.** Data collection and refinement statistics of the AF17121•IL-5Rα complex

| | |
|---|---|
| **Processing** | |
| Diffraction source | Beamline MX1–3 PETRA III, DESY (Hamburg) |
| Wavelength (Å) | 0.9796 |
| Space group | $P6_422$ |
| Unit cell | $a = b = 138.06$ Å, $c = 145.86$ Å, $\alpha = \beta = 90°$, $\gamma = 120°$ |
| Resolution (Å) | 43.2–2.75 (2.85–2.75) |
| Number of reflections (total) | 322,031 (32,943) |
| $R_{pim}$ | 0.039 (0.731) |
| $CC_{1/2}$ | 0.928 (0.615) |
| $I/\sigma I$ | 13.6 (2.0) |
| Completeness (%) | 99.9 (99.7) |
| Redundancy | 14.7 (15.5) |
| **Refinement** | |
| Resolution (Å) | 43.2–2.75 (2.85–2.75) |
| Number of reflections | 21,878 (2119) |
| $R_{work}/R_{free}$ (%) | 20.2 (33.6)/22.6 (36.7) |
| FOM | 0.81 (0.72) |
| TLS groups | 2 (group 1: IL-5Rα Lys7–Arg315; group 2: AF17121 Val1–Glu18) |
| Number of atoms | |
| Protein | 2637 (327 residues) |
| Water | 24 |
| Average *B* factors | |
| Protein (Å$^2$) | 106.2 |
| Water (Å$^2$) | 91.3 |
| RMSD | |
| Bond lengths (Å) | 0.003 |
| Bond angles (°) | 0.91 |
| Ramachandran analysis[a] | |
| Favored (%) | 93.5 (306 of 327 residues) |
| Outliers (%) | 1.9 (6 of 327 residues) |
| Clashscore[b] | 7.5 |
| Rotamer outliers (%) | 1.4 (4 of 327 residues) |

Values in parentheses are for the highest resolution shell.
[a] As reported by MolProbity analysis.
[b] As reported by Phenix version 1.9.1692, calculated as 1000 × (number of bad overlaps/number of atoms).

## Results

### AF17121 blocks IL-5 by binding IL-5Rα in an overlapping epitope

We have crystallized the complex of the cyclic peptide AF17121 bound to the ectodomain of IL-5Rα and determined the structure to 2.75 Å resolution (Table 1). Density maps revealed one complex in the asymmetric unit (Fig. 1A, Fig. S1). For IL-5Rα, residues Lys7 to Arg313 were observed, which group into three fibronectin type III-like domains (termed D1, D2 and D3) that together form a wrench-like receptor architecture as in IL-5•IL-5Rα [18]. In contrast to IL-5Rα, the 18mer peptide exhibits little secondary structure. The cyclic loop constrained by the disulfide bond between Cys4 and Cys15 comprises two short strands (Trp5–Ile7, Thr12–Phe14) linked by a sharp 4-residue β-turn (Fig. 1B). AF17121 snugly fits into in the cleft formed by domains 1 (residues 7–101) and 2 (residues 102–217) of IL-5Rα (Fig. 1C). AF17121 strand 1 forms three main chain-main chain hydrogen bonds with strand 5 in IL-5Rα D1, thereby extending the lower three-stranded β-sandwich of IL-5Rα D1 (strands 1, 2 and 5), with the two-stranded β-sheet of AF17121 yielding a twisted five-stranded intermolecular β-sheet. A comparison shows that although peptide and IL-5 share an overlapping epitope at IL-5Rα D1 and D2, both ligands are differently located in the wrench-like cleft of IL-5Rα, with AF17121 being deeper immersed in the receptor cleft [18] (Fig. 1C, D). Furthermore, AF17121 shares no contacts with IL-5Rα D3 (residues 218–315), while IL-5 binding requires all three domains of IL-5Rα [18] (Fig. 1E, F). The tight integration of the peptide into the IL-5Rα D1D2-cleft becomes apparent upon analyzing the contact areas, showing that 40% of the peptide's surface (820 Å$^2$ out of 2075 Å$^2$ total surface area) share contact with IL-5Rα, whereas only 11% of the IL-5 surface (1290 Å$^2$ out of 11,440 Å$^2$ total surface area) participate in the interface to IL-5Rα [18]. The large contact between AF17121 and IL-5Rα provides first hints as to why the peptide can bind with high affinity ($K_D$ AF17121–IL-5Rα$_{ECD}$: 90 ± 4.5 nM), which is only 150-fold lower than binding of IL-5 to IL-5Rα ($K_D$ IL-5–IL-5Rα$_{ECD}$: $K_D$ 0.58 ± 0.18 nM). It had been initially

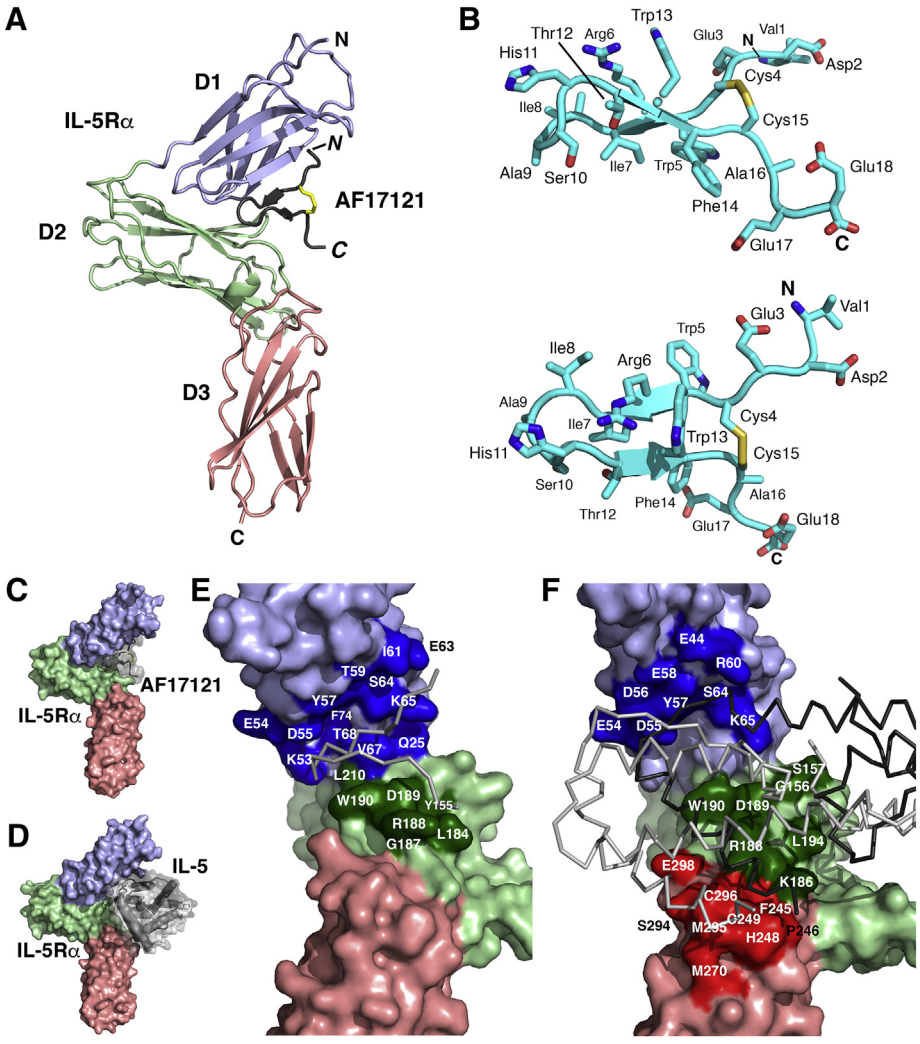


**Fig. 1.** The IL-5 inhibitory peptide AF17121 bound to the IL-5Rα ectodomain. (A) The complex AF17121•IL-5Rα is shown as ribbon plot. The FNIII domains D1, D2 and D3 are marked in blue, green and red, respectively; the peptide is shown in gray. The disulfide bond of the cyclic peptide is shown as yellow sticks. (B) Detailed view of AF17121, which consists of a two-stranded, anti-parallel β-sheet with two short strands (β1: Trp5–Ile7; β2: Thr12–Phe14). (C) Surface representation of AF17121•IL-5Rα showing the 18mer peptide (gray) within its binding cleft of the IL-5Rα wrench architecture. (D) As in panel C but for IL-5•IL-5Rα. IL-5 occupies a larger, yet overlapping epitope at IL-5Rα. (E) Enlarged view of the binding epitope of AF17121 at IL-5Rα. Residues buried upon complex formation are indicated in darker colors. One-letter code is used for amino acid labeling. (F) As in panel E but for IL-5•IL-5Rα.

proposed that AF17121 resembles the two-stranded β-sheet of IL-5 and hence mimics IL-5 [14]. The structures of AF17121•IL-5Rα and IL-5•IL-5Rα now proves this model to be wrong. While the β-sheet of AF17121 forms an extended intermolecular β-sheet with the lower three-stranded β-sheet of domain D1, the β-sheet of IL-5 extends the upper four-stranded β-sheet of IL-5Rα D1 (Fig. 2A, B). Thereby, AF17121's two-stranded β-sheet is “displaced” of by about 10–12 Å compared to the β-sheet of IL-5 shifting it from a peripheral site to a position closer to the D1D2 hinge of the wrench (Fig. 2C). Despite the different placement of AF17121 at IL-5Rα, which leads to AF17121 and IL-5 barely sharing overlapping backbone atom positions, the AF17121•IL-5Rα structure explains as to how the peptide can effectively compete off IL-5 from binding to IL-5Rα. While not mimicking the binding of IL-5, AF17121, however, utilizes key residues of IL-5Rα essential for IL-5 binding (see below) and thus blocks these from interaction with IL-5.

### A protected intermolecular salt bridge is the key element for binding of AF17121 to IL-5Rα

Inspection of the AF17121•IL-5Rα interface revealed additional polar bonds between peptide and receptor (Fig. 3 and Table S1). A hydrogen bond (h-bond) was found between the N-terminus of

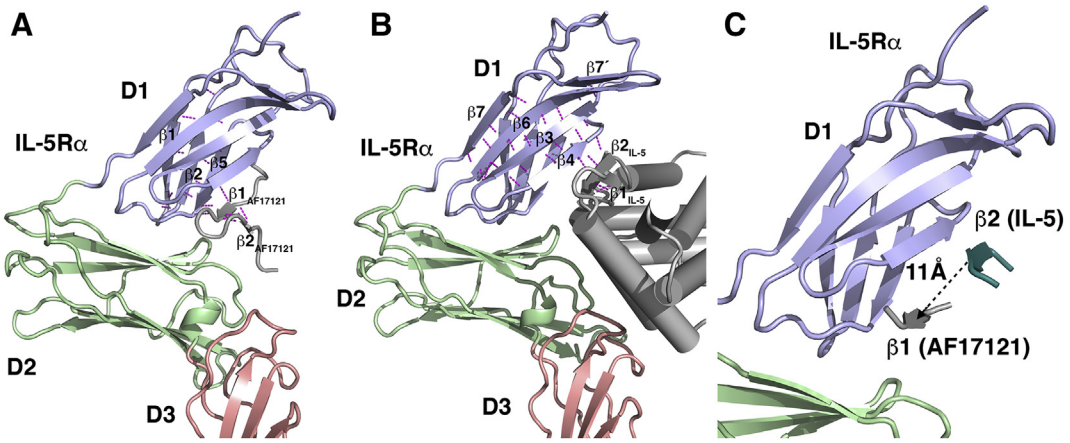


**Fig. 2.** AF17121 and IL-5 occupy different position in the IL-5Rα interface. (A) While both AF17121 and IL-5 (B) form an intermolecular β-sheet with the β-sandwich of IL-5Rα domain 1 (h-bonds are indicated as magenta stippled lines), position and orientation of the β-strand contributed by AF17121 and IL-5 differ. (A) AF17121 forms a sheet with the lower three-stranded β-sheet of domain 1 of IL-5Rα with strand β1 of AF17121 running parallel to IL-5Rα strand 5. (B) In IL-5•IL-5Rα, strand 2 of IL-5 engages in an intermolecular β-sheet with the upper four-stranded β-sheet of IL-5Rα domain 1 with IL-5 strand 2 running anti-parallel to strand 4 of IL-5Rα. (C) While forming a similar interaction, the β-strands of both ligands occupy significantly different positions and are offset by about 11 Å.

AF17121 and the carboxylate group of IL-5Rα Glu63 (Fig. 3A). The negative charge of Glu3 (AF17121) potentially engages in a coulombic interaction with Lys65 of IL-5Rα (Fig. 3A). An exchange of Asp2 and Glu3 of AF17121 with alanine indeed resulted in a 13-fold decrease in binding, suggesting that the acidic residues are involved in polar interactions with IL-5Rα [14,16]. The peptide's C-terminus is also fixated by three h-bonds between the carboxylate group of AF17121 Glu17 and IL-5Rα Arg188 as well as Tyr155 (Fig. 3B). Accordingly, exchange of Glu17 and Glu18 with alanine attenuated IL-5Rα binding about 10-fold [14,16]. However, the significance of AF17121 N- and C-terminus possibly differs, as binding analysis showed that mutation D2A/E3A mainly affects peptide–receptor association, while mutation E17A/E18A increased dissociation of the peptide from the complex [16]. Computational analysis of the charge distribution of AF17121 and IL-5Rα indicates indeed a highly complementary surface potential with AF17121 Asp2 and Glu3 opposite to a positively charged patch around IL-5Rα Lys65 and AF17121 Glu17 and Glu18 being close to a positive patch formed by IL-5Rα Lys186, Arg188 and Arg297 (Fig. S2). Since an AF17121 variant with all acidic residues mutated still binds IL-5Rα albeit with reduced affinity, the four acidic residues do not represent the hot spot of binding of the peptide–receptor interaction [16].

The most notable interaction between peptide and IL-5Rα is a bi-dentate salt bridge formed between Arg6 of AF17121 and IL-5Rα Asp55 (Fig. 3C). Both side chain groups are oriented planar and tightly shielded from solvent by surrounding residues, that is, AF17121 Ile8, His11 and Trp13 as well as IL-5Rα Tyr57 (Fig. 3C). The importance of Arg6 was previously highlighted as its replacement with alanine strongly impaired peptide–receptor interaction [14,16]. Moreover, a positive charge alone at position 6 of the peptide is not sufficient, but a guanidinium group at the correct distance from the backbone is required for high-affinity binding [17]. Thus, it has been proposed that AF17121 Arg6 mimics Arg91 of IL-5 [19], which is known from the IL-5•IL-5Rα structure to likewise interact with IL-5Rα Asp55 [18,20]. A comparison now shows that the interaction of both arginine residues with IL-5Rα fundamentally differs. Arg91 is one of three arginines in IL-5, that is, Arg32, Arg90 and Arg91, that engage in multiple polar bonds with acidic counterparts at IL-5Rα (Glu44, Asp55, Asp56 and Glu58) forming an interwoven polar zipper [18]. In contrast, Arg6 is the only arginine in AF17121 and forms an isolated bi-dentate salt bridge with Asp55 (Fig. 3C). While the side chain of Arg91 is positioned through intramolecular polar bonds formed with other residues of IL-5, for example, Glu44 and Gln95, Arg6 of AF17121 is positioned through van der Waals contacts with the residues of the peptide and receptor. Noteworthy, three of the four surrounding residues are of aromatic nature. IL-5Rα Tyr57 is arranged planar above the Arg6′ guanidinium group and the indole ring of AF17121 Trp13 is at the side oriented perpendicular to the arginine head group (Fig. 3C). Thus, the intermolecular salt bridge is immersed in two ππ electron stacking interactions, which likely potentiate this polar interaction. The mutation W13A indeed resulted in 13-fold decrease in receptor binding. When Trp13 was substituted for unnatural amino acids with larger aromatic systems, such as 1-

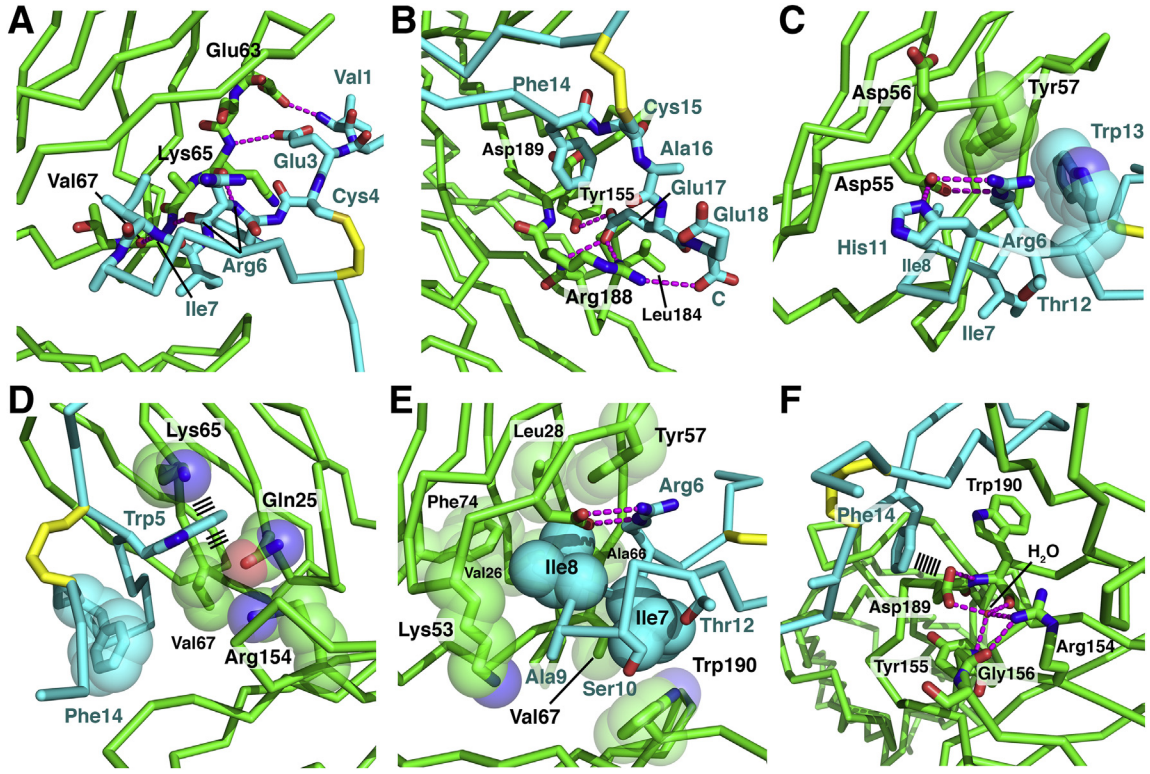


**Fig. 3.** Polar and hydrophobic interactions in the AF17121•IL-5Rα interface. (A) Detailed view of polar bonds (magenta stippled lines) between the N-terminal residues of AF17121 (C-atoms cyan), for example, Val1, Glu3, and the main chain–main chain h-bonds of AF17121 strand 1 with IL-5Rα (C-atoms green). (B) Polar bonds between the C-terminus of AF17121 and IL-5Rα. AF17121 Glu17 engages in three h-bonds with residues of IL-5Rα, that is, Tyr155 OH, Arg188 $NH_{bb}$ and Arg188 NH2. A polar bond is potentially formed between the AF17121 C-terminus and IL-5Rα Arg188 NH2. (C) The bidentate salt bridge between AF17121 Arg6 and IL-5Rα Asp55 is the key determinant of peptide–receptor interaction. It is immersed in ππ-stacking interactions with AF17121 Trp13 (transparent van der Waals spheres) and IL-5Rα Tyr57. AF17121 His11 coordinates IL-5Rα Asp55 and shields the Arg6–Asp55 interaction. (D) Hydrophobic and ππ-stacking (indicated by parallel lines) interactions are also found in AF17121•IL-5Rα. (E) AF17121 Ile7 and Ile8 make hydrophobic contacts with residues of IL-5Rα. Ile7 is packed between IL-5Rα Val67 and Trp190. Ile8 makes a knob-into-hole interaction with IL-5Rα Val26, Leu28, Ala66 and Phe74. (F) AF17121 Phe14 forms a ππ-stacking interaction with IL-5Rα Asp189, which is shielded by Trp190. Details about intermolecular hydrogen bonds are found in Table S1.

or 2-naphtylalanine, β-3-benzothienyl-L-alanine or 4-benzoyl-L-phenylalanine binding to IL-5Rα was either slightly improved (i.e., 1-naphtylalanine) or attenuated, indicating that not only size but also configuration of the aromatic system matters [17]. The imidazole ring of AF17121 His11 opposite of Trp13 completes the entrapment of the Arg6–Asp55 salt bridge (Fig. 3C). It further coordinates Asp55 via an h-bond between the imidazole nitrogen and the aspartate carboxylate group. Its significance for the peptide–receptor interaction is documented from the mutation H11A, which results in 10-fold loss in binding [16].

Several hydrophobic residues of AF17121 also share contacts with IL-5Rα and might thus contribute to binding. More than 60% of the accessible surface of the peptide residues Trp5, Ile7, Ile8 and Phe14 become buried upon complex formation, with Trp5 and Ile8 sharing the largest contact of about 130 $Å^2$ each (Fig. 3D–F). Despite their large interfaces, these four residues contribute very differently to binding. Alanine scanning showed that Trp5 and Ile8 are not significant for binding, while mutation I7A and F14A decreased affinity to IL-5Rα 18- and 10-fold, respectively [17]. Structure analysis does not explain this discrepancy. While the importance of Phe14 might be explained with its ππ-stacking interaction with the carboxylate group of IL-5Rα Asp189 (Fig. 3F), W5A has no consequences for IL-5α binding, although Trp5 engages in a similar interaction with IL-5Rα Gln25 (Fig. 3D). Similarly, AF17121 Ile8 makes a seemingly perfect knob-into-hole interaction with a hydrophobic cleft formed by Leu28, Ile49, Tr57, Thr68 and Phe74 in IL-5Rα, but upon mutation to alanine, binding affinity is unaltered [17]. On the contrary, AF17121 I7A resulted in a major drop in binding to IL-5Rα, although Ile7 participates in similar contacts with IL-5Rα Val45 and Trp190 (Fig. 3E).

In summary, a salt bridge between AF17121 Arg6 and Asp55 of IL-5Rα presents the key determinant for the strong peptide–receptor interaction and forms the basis for the highly effective inhibition of IL-5 binding and receptor activation. The surprisingly high effectiveness is likely due to the peculiar environment of this polar interaction, which leads to a potentiation of these few hydrogen bonds.

### Recognition and binding mechanism of IL-5Rα differ for AF17121 and IL-5

To identify possible differences in the binding of AF17121 and IL-5, 26 IL-5Rα variants investigating 21-amino-acid positions located in the binding interface were produced and analyzed side-by-side by surface plasmon resonance (SPR; Fig. 4 and Table S2). Of the 15 alanine mutants tested in IL-5Rα domain 1, only 7 showed a ≥5-fold loss in peptide binding. Among those are Asp55 and Tyr57, which are involved in the intermolecular peptide–IL-5Rα salt bridge (see above; Fig. 4A). Mutation of either residue to alanine severely impaired binding of AF17121 to IL-5Rα. Here, an aspartate at position 55 of IL-5Rα was essential as an isosteric asparagine or a larger glutamate could not rescue binding. In contrast, the latter mutations, D55N and D55E, did not fully abrogate binding of IL-5 and led to only about 5-fold decrease in affinity (Table S2). This difference can be explained by the less tightly packed interface and the fact that only one intermolecular h-bond is formed between IL-5Rα Asp55 and IL-5 Arg91 allowing to accommodate similar amino acid types. The opposite is seen when replacing IL-5Rα Tyr57 with different aromatic residues. While AF17121 binding was not affected by the IL-5Rα mutations Y57F and Y57W, IL-5 binding was decreased 2- to 3-fold (Table S2). Also, neighboring residues showed different effects. Mutation of Asp56 and Glu58, which are part of the polar zipper in IL-5•IL-5Rα and strongly contributed to IL-5 binding [18], did not alter peptide binding (Fig. 4 and Table S2).

Four more residues in domain 1 of IL-5Rα, that is, Ile49, Lys65, Val67 or Phe74 attenuated peptide binding by more than 5-fold. For I49A and F74A (but not for V67A), a large drop in binding was also observed for IL-5 (~83-fold for I49A and ~88-fold for F74A). As neither residue shares contact with IL-5, we assume that I49A and F74A (as well as P52A) leads to conformational changes within D1 β-strand 4, which then indirectly affect ligand binding. Mutation K65A in IL-5Rα decreased AF17121 binding confirming the interactions between the acidic N-terminus of the peptide (Fig. 4A), namely, Asp2 and Glu3, and the lysine residue. Since IL-5Rα Lys65 does not contact IL-5 in IL-5•IL-5Rα [18], K65A did not affect IL-5 binding, supporting the hypothesis that the functional epitopes for AF17121 and IL-5 differ (Fig. 4A, B). Noteworthy, alanine substitution of a couple of IL-5Rα residues, for example, Lys53 and Glu63, increased affinity specifically for the peptide (Fig. 4A). Variant K53A showed the largest increase with a 5-fold lower $K_D$ as for wild-type IL-5Rα. As Lys53 shares contacts with the β-turn of AF17121, namely, residue Ala9, removal of the large side chain likely facilitates binding due to reduced steric hindrance. Alanine

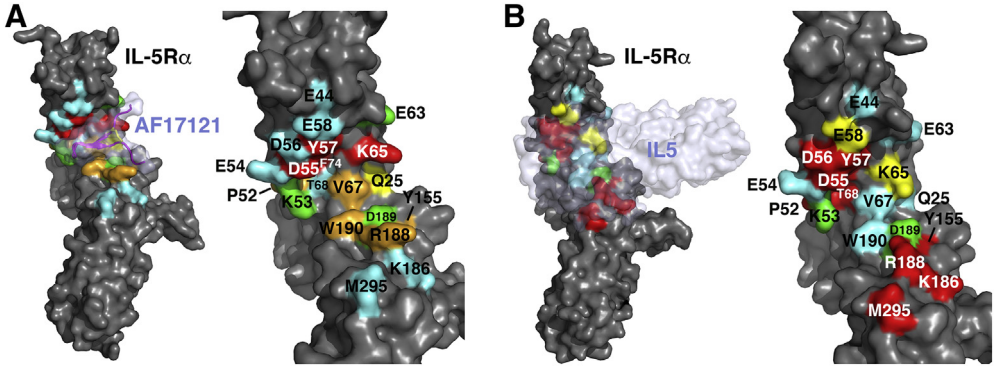


**Fig. 4.** Functional epitopes of AF17121 and IL-5 at IL-5Rα differ. The contribution of residues of IL-5Rα to binding of AF17121 (A) or IL-5 (B) was determined by mutagenesis and interaction analysis. (A, left panel) Surface representation of IL-5Rα, the peptide binding site is indicated, AF17121 is shown as ribbon plot with transparent surface. (A, right panel) Enlarged view of the interface with residues color-coded according to their contribution to binding of AF17121. Residues in cyan do not alter binding upon mutation to alanine (change in $K_D$ < 2-fold), residues in yellow alter binding, but exhibit a $\Delta\Delta G \leq 2.4$ kJ mol$^{-1}$. Residues in orange contribute ≥2.4 but ≤5 kJ mol$^{-1}$, and residues in red have a $\Delta\Delta G \geq 5$ kJ mol$^{-1}$. A few residues showed improved ligand binding upon mutation to alanine ($\Delta\Delta G \geq -1$ kJ mol$^{-1}$) and are marked in green. (B) as in panel A but for the analysis of binding of IL-5. Details about the SPR data underlying the color coding are provided in Tables S2A and S2B.

replacement of IL-5Rα Glu63, which is close to the acidic N-terminus of AF17121, that is, Asp2 and Glu3, also improved binding by 2-fold. Here, the removal of the negative charge in IL-5Rα E63A decreases electrostatic repulsion.

Most of the binding interface for AF17121 resides in IL-5Rα domain 1 and only few residues in domain 2 engage in polar or van der Waals interaction with the peptide. Five residues in IL-5Rα D2, that is, Tyr155, Lys186, Arg188, Asp189 and Trp190, were exchanged for alanine and their binding was analyzed (Fig. 4A, B and Table S2). Y155A decreased peptide binding by 6-fold highlighting the importance of the h-bond between Tyr155 and AF17121 Glu17. IL-5Rα K186A showed strongly decreased IL-5 binding (14-fold), but the mutation had no significant effects on AF17121 binding, consistent with the structure showing no contacts between Lys186 and peptide. In contrast, alanine replacement of Arg188, whose guanidinium group forms h-bonds with AF17121 C-terminus and Glu17, decreased affinity for the peptide 4-fold. Unexpectedly, peptide binding was unaffected for the variant R188K, indicating that a positive charge is solely sufficient for IL-5Rα–peptide interaction and no particular chemical architecture is required. This is different from IL-5 binding. Here, IL-5Rα Arg188 forms an intramolecular h-bond with Cys296 to stabilize the β6β7-loop in the receptor domain 3. As this loop is in contact with IL-5, its destabilization strongly decreases IL-5 binding (R188A ~50-fold), which is not rescued by the mutation R188K (affinity loss ~130-fold) as lysine is too short to maintain this h-bonding (Fig. 4B and Table S2). A third mutation positively affecting AF17121 binding was IL-5Rα D189A (about 1.5-fold), although the structure suggested that Asp189 would favorably interact with AF17121 Phe14 through ππ-stacking interactions. Possibly, the close contact of Asp189 with Phe14 severely restricts its side-chain conformation, which is energetically unfavorable explaining the gain in binding energy upon exchange with a smaller alanine. The fifth residue investigated in IL-5Rα domain 2, Trp190, makes important hydrophobic contacts with AF17121 Ile7. Conformingly, mutation W190A exhibited decreased peptide binding (3-fold), while affinity for IL-5 was unaffected (Fig. 4A, B).

In summary, the results clearly show that the two structurally distinct IL-5Rα ligands, AF17121 and IL-5, are recognized and bound differently, although a

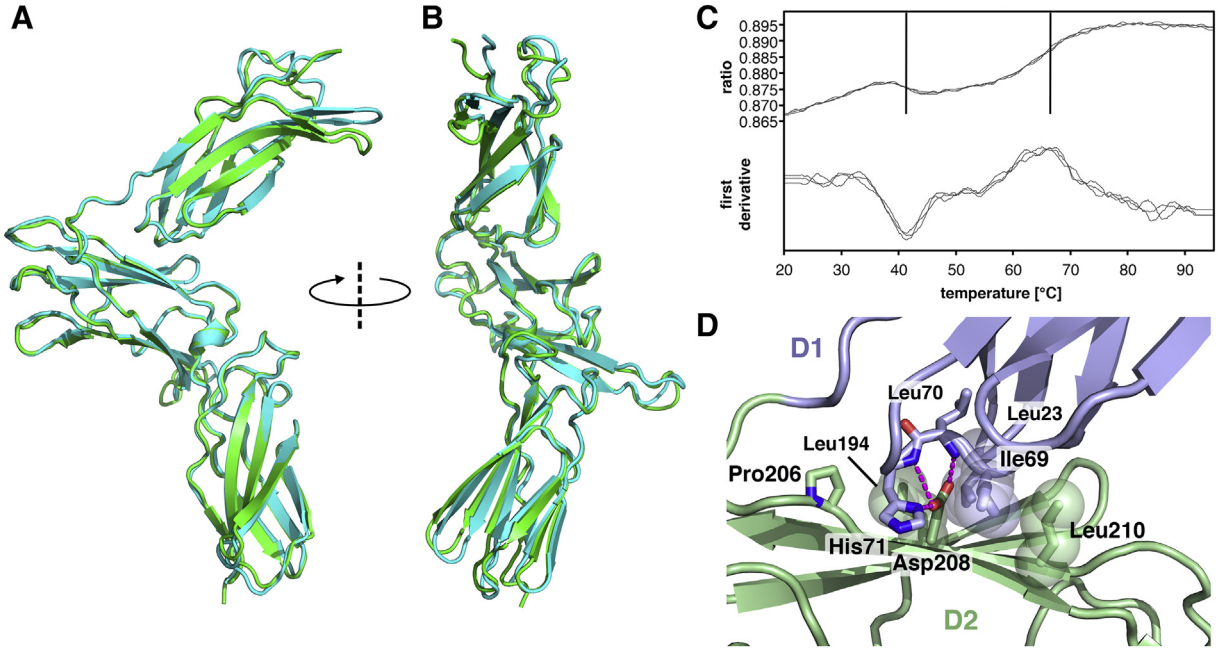


**Fig. 5.** The IL-5Rα ectodomain structure is unaltered when bound to the vastly different ligands AF17121 and IL-5. (A) The structures of IL-5Rα bound to AF17121 (green) and IL-5 (cyan) can be superimposed almost perfectly, indicating that IL-5Rα does not adapt to the different structures of the ligands, AF17121 and IL-5. (B) As in panel A but rotated 90° clockwise around the *y*-axis. (C) While this finding suggests a rigid, fixed IL-5Rα architecture, further analyses indicated a flexible IL-5Rα ectodomain. A differential scanning fluorimetry showed two transitions (minimum and maximum of the first derivative are marked by vertical lines) indicative of two melting temperatures, that is, 42 ± 0.4 °C and 66 ± 1.2 °C. (D) Stability of the wrench architecture and its impact on ligand binding was tested by mutagenesis. Leu23, Ile69, His71, Leu194, Pro206, Asp208 and Leu210 of IL-5Rα were exchanged to alanine, and binding of AF17121 and IL-5 to these variants was analyzed. To test whether a fixed architecture impedes binding of AF17121 or IL-5, the h-bonds between Leu70 and His71 and Asp208 were replaced with a disulfide bond. Two IL-5Rα double variants were generated, with Ile69 and Asp208 or His71 and Asp208 being replaced with cysteines. For details of the analysis, see Table 2.

seemingly identical interaction pairing, that is, AF17121 Arg6—IL-5Rα Asp55 and IL-5 Arg91—IL-5Rα Asp55, suggested otherwise at first (Fig. S3). Thus, IL-5 neutralization by the peptide AF17121 results less from direct competition for the very same residues in IL-5Rα, but the implementation of a steric hindrance to block IL-5 from accessing its binding site.

### Is the IL-5Rα wrench architecture prefixed or formed upon ligand binding by a selection-fit mechanism?

Previously, we hypothesized that the wrench-like architecture of the IL-5Rα ectodomain might be preformed and fixed [18]. A rigid receptor architecture would, however, also bear consequences for rational structure-based design of small-molecule- or peptide-based IL-5 competitors such as AF17121. We were thus puzzled that the structures of IL-5Rα of the complexes AF17121•IL-5Rα and IL-5•IL-5Rα could be superimposed almost perfectly (r.m.s.d. about 1.4 Å for the Cα-atoms of residues 7 to 313; Fig. 5A, B). While an identical architecture when bound to two structurally vastly different ligands seemingly confirms the above-described hypothesis, additional data indicated ligand binding via a flexible selection fit mechanism. First, a thermal shift assay for IL-5Rα to identify conditions that facilitate crystallization of "free" IL-5Rα yielded a surprisingly low "melting" temperature of only 35 °C, 2 °C below the physiological temperature. Second, a van't Hoff analysis of the temperature dependency of IL-5–IL-5Rα SPR binding data revealed a clear non-linear correlation of $\ln(K_D)$ *versus* $1/T$ (despite a small temperature range of 15 °C to 35 °C) hinting toward a conformational rearrangement during binding (Fig. S4). We therefore investigated the conformational flexibility using differential scanning fluorescence spectroscopy employing a Prometheus NT.48 device (NanoTemper). To our surprise, this analysis yielded two melting temperatures: 42 ± 0.4 °C and 66 ± 1.2 °C (Fig. 5C), suggesting that the ectodomain of IL-5Rα unfolds stepwise. The first transition hereby possibly represents a local opening of the wrench architecture, while the second transition at high temperature corresponds with a global unfolding of IL-5Rα. These data point toward a selection fit binding mechanism, in which the ligand binds to a partially open architecture that upon closing into the conformationally highly defined wrench structure becomes stabilized by additional intramolecular interactions in the D1–D2 interface.

We tested whether the peptide AF17121 and IL-5 require different flexibility and generated IL-5Rα variants with mutations in the D1–D2 interface that potentially modulate the flexibility of the wrench architecture (Fig. 5D). Their impact on AF17121 and IL-5 binding was analyzed by SPR to provide information on binding kinetics (Table 2). Of the seven mutations investigated, L194A and P206A did affect binding of neither the peptide nor of IL-5. The IL-5Rα variants L23A (5-fold) and I69A (2.6-fold) had slightly decreased affinities for AF17121, while IL-5 binding was only impaired for L23A (2-fold). Three further IL-5Rα variants, that is, H71A, D208A and L210A, showed strongly attenuated (or no) binding to peptide and IL-5. This can be explained by the fact

**Table 2.** SPR interaction analysis of IL-5Rα variants with mutations affecting the wrench-like architecture

| AF17121 | | receptor variant | IL-5 | |
|---|---|---|---|---|
| rel. $K_D$ | $\Delta\Delta G$ [kJ mol$^{-1}$] | | rel. $K_D$ | $\Delta\Delta G$ [kJ mol$^{-1}$] |
| 1.0 (= 90 ± 4.5 nM) | - | wildtype | 1.0 (= 0.58 ± 0.18 nM) | - |
| 5.0 | 4.0 | L23A | 2.2 | 2.0 |
| 2.6 | 2.4 | I69A | 1.2 | 0.43 |
| 6.8 | 4.7 | H71A | 19.0 | 7.3 |
| 0.97 | -0.08 | L194A | 0.95 | -0.13 |
| 0.90 | -0.26 | P206A | 1.0 | 0 |
| 22.2 | 7.7 | D208A | 19.0 | 7.3 |
| 58.9 | 10.1 | L210A | 62.1 | 10.2 |
| **fixed wrench variants** | | | | |
| 0.88 | -0.32 | I69C/D208C | 84.5 | 11.0 |
| 31.4 | 8.5 | H71C/D208C | 32.8 | 8.7 |

$\Delta\Delta G$ was calculated from $\Delta\Delta G = -RT \ln(K_D[\text{WT}]/K_D[\text{variant}]$, with $R$ = 8.314 J mol$^{-1}$ and $T$ = 298 K. Variants with a change in $K_D$ <2-fold are marked in cyan, variants with a change in $K_D \geq$ 2-fold and $\Delta\Delta G$ values <2.4 kJ mol$^{-1}$ are yellow, variants with $\Delta\Delta G \geq$ 2.4 and < 5 kJ mol$^{-1}$ are orange, variants with $\Delta\Delta G \geq$ 5 kJ mol$^{-1}$ are highlighted in red. Mean values and standard deviation for $K_D$, association $k_{on}$ and dissociation $k_{off}$ rate constants are provided in Table S3.

that h-bonds formed between Asp208 (domain D2) and Leu70 as well as His71 (domain 1), together with the shielding provided by Leu210, are essential for IL-5Rα to adopt its wrench-like architecture upon ligand binding. SPR analysis also showed that whenever peptide and/or IL-5 binding to these IL-5Rα variants was decreased, it was due to slower association, while dissociation remained unaffected (Table S3). This suggests that folding of IL-5Rα into its wrench architecture becomes the rate-limiting step. Given the different size of AF17121 and IL-5, it seemed puzzling that both ligands require similar ectodomain flexibility for binding. We therefore engineered two IL-5Rα double variants, that is, I69C/D208C and H71C/D208C, in which two residues lying face-to-face in the D1–D2 interface were replaced with cysteines sufficiently close for intramolecular disulfide formation (Fig. 5D). This disulfide bond would constrain D1–D2 domain orientation such that the wrench-like architecture becomes rigidified. Consistent with our idea that a fully rigid wrench architecture would present a steric burden for binding to the large IL-5, we found that interaction with both variants was dramatically impaired (Table 2). In contrast, binding of AF17121 to IL-5Rα I69C/D208C occurred with wild-type-like affinity and only binding to H71C/D208C was attenuated (Table 2). This suggests that the larger IL-5 requires a considerably larger opening of the IL-5Rα wrench for binding than the peptide AF17121, whose binding epitope is located mainly within domain 1 of IL-5Rα.

### Optimizing AF17121 toward improved IL-5Rα binding and inhibition

While AF17121 binds IL-5Rα remarkably strong, its potential use *in vivo* as IL-5 inhibitory therapeutic still requires (too) high concentrations to be effective. We therefore aimed for structure-based design of AF17121 variants showing improved binding to IL-5Rα, possibly translating into improved inhibition of IL-5 signaling. A prokaryotic expression scheme was established using a fusion-protein approach in which the peptide was fused to a chemically activatable protease [21]. The peptide was cleaved off through intramolecular proteolysis resulting in peptides that, compared to chemically synthesized AF17121, comprised only one additional methionine and an additional leucine at the N- and C-terminus, respectively. The recombinantly derived AF17121 exhibited affinities to IL-5Rα basically identical to chemically synthesized peptide. Based on our structure, 11 positions in the peptide were chosen and replaced by different amino acid types to yield a total of 21 variants. As AF17121 Arg6 and Trp13 were investigated in several studies in the past [19], both residues were not tested in our mutagenesis study. Binding to IL-5Rα was analyzed by microscale thermophoresis (MST) at 25 °C and 37 °C to test whether the known flexibility of the IL-5Rα architecture modulates peptide binding in a site-specific manner (Tables 3 and S4).

Particular emphasis was drawn to the hydrophobic and ππ-stacking interactions between peptide and receptor. *In silico* simulations suggested that the hydrophobic contacts of AF17121 Ile7 and Ile8 could be possibly improved. However, exchange of Ile7, which is located above Trp190 of IL-5Rα, with larger amino acids (e.g., I7F, I7Y, I7H, I7M) resulted in a strongly reduced binding to IL-5Rα (Table 3). Similarly, replacement of Ile8 with larger amino acids such as phenylalanine or methionine decreased binding 94- and 189-fold instead. Thus, steric hindrance likely introduced with these larger amino acids overcompensates the assumed increased hydrophobic interactions. Two residues of AF17121, Trp5 and Phe14, engage in potentially favorable ππ-stacking interactions with the carboxamide and carboxylate groups of IL-5Rα Gln25 and Asp189, respectively. While mutation Q25A in IL-5Rα slightly decreased peptide binding consistent with favorable ππ-stacking interactions, D189A showed an increased affinity for AF17121 (Table S2). The corresponding mutations in AF17121, that is, W5Y and F14W showed mixed results. For variant W5Y receptor binding was attenuated 4-fold, indicating that a smaller aromatic ring decreases peptide binding. Introducing a larger tryptophan for Phe14 led to a slight, albeit statistically not significant increase in receptor binding (Table 3). We also tested whether mutation of residues in the short termini can enhance IL-5Rα binding. AF17121 Glu3 is in close to IL-5Rα Glu63, whose mutation to alanine led to a 2-fold increased affinity (Table S2). AF17121 Glu3 was replaced with a glutamine to remove the negative charge and to maintain side-chain chemistry for possible polar interactions. No significant increase in affinity was observed for E3Q, though (Table 3). In the C-terminus, Ala16 was mutated to glycine and proline, and Glu17 was exchanged for aspartate to possibly improve the h-bond network seen between Glu17 and IL-5Rα residues Tyr155, Arg188 and Asp189. Interaction analyses did not reveal an increase in binding. While residues in AF17121's sharp β-turn share little contact with IL-5Rα, these residues might nevertheless affect binding due to folding the β-sheet loop structure. Hence, Ala9, Ser10, His11 and Thr12 were exchanged with different amino acids. AF17121 variants A9F, T12Q and T12E, albeit *in silico* promising additional interactions with IL-5Rα, did neither improve nor attenuate binding significantly (Table 3). Exchanging His11 with either lysine or arginine, which should yield additional polar interactions with IL-5Rα Glu54 or Asp56, significantly decreased affinity. AF17121 Ser10 does not engage in polar contacts and also shares only little contact with IL-5Rα. However, being located at the

**Table 3.** Interaction analysis of AF17121 variants employing MST and inhibition of IL-5-mediated TF1 cell proliferation

| AF17121 and variants | rel. $K_D$ 25°C | ΔΔG at 25°C [kJ mol$^{-1}$] | rel. $K_D$ 37°C | ΔΔG at 37°C [kJ mol$^{-1}$] | $K_i$ [nM] | rel. $K_i$ |
|---|---|---|---|---|---|---|
| **wildtype** | 1.0 (= 84.8 nM) | - | 1.0 (= 39.9 nM) | - | 49.5 ± 16.1 | - |
| **E3Q** | 0.97 | -0.07 | 0.85 | -0.40 | 17.9 ± 6.2 | 0.4 |
| **W5Y** | 4.3 | 3.6 | 6.1 | 4.7 | ND | - |
| **I7F** | 7.4 | 4.9 | 16 | 7.2 | ND | - |
| **I7H** | 4.4 | 3.7 | 9.5 | 5.8 | ND | - |
| **I7M** | 3.7 | 3.3 | 5.8 | 4.5 | ND | - |
| **I7Y** | 3.2 | 2.9 | 14 | 6.9 | ND | - |
| **I8F** | 94 | 11 | 147 | 13 | ND | - |
| **I8M** | 189 | 13 | 115 | 12 | ND | - |
| **I8V** | 1.5 | 1.0 | 2.0 | 1.8 | 22.8 ± 12.4 | 0.5 |
| **A9F** | 0.98 | -0.05 | 1.1 | 0.11 | 49.8 ± 13.4 | 1.0 |
| **S10A** | 0.29 | -3.0 | 0.22 | -3.9 | 28.2 ± 13.5 | 0.6 |
| **S10G** | 5.0 | 4.0 | 13 | 6.6 | 321 ± 33.9 | 6.5 |
| **S10P** | 32 | 8.6 | 97 | 12 | ND | - |
| **H11K** | 6.5 | 4.6 | 8.9 | 5.6 | ND | - |
| **H11R** | 2.7 | 2.5 | 3.8 | 3.5 | 49.9 ± 22.2 | 1.0 |
| **T12E** | 1.3 | 0.69 | 1.6 | 1.2 | 56.0 ± 19.3 | 1.1 |
| **T12Q** | 1.6 | 1.1 | 2.4 | 2.3 | 76.3 ± 22.4 | 1.5 |
| **F14W** | 0.72 | -0.80 | 0.81 | -0.54 | 40.8 ± 9.8 | 0.8 |
| **A16G** | 0.82 | -0.50 | 1.0 | 0 | 24.1 ± 7.9 | 0.5 |
| **A16P** | 0.97 | -0.08 | 1.2 | 0.46 | 30.5 ± 7.4 | 0.6 |
| **E17D** | 0.89 | -0.29 | 1.1 | 0.30 | 31.3 ± 6.2 | 0.7 |

$\Delta\Delta G$ was calculated from $\Delta\Delta G = -RT \ln(K_D[\text{WT}]/K_D[\text{variant}]$, with $R$ = 8.314 J mol$^{-1}$ and $T$ = 298 K (25 °C) or 310 K (37 °C). ND, not determined. AF17121 variants with $\Delta\Delta G \geq 2.4$ and <5 kJ mol$^{-1}$ are marked in orange, variants with $\Delta\Delta G \geq 5$ kJ mol$^{-1}$ are red, variants with improved binding (threshold $\Delta\Delta G = -0.5$ kJ mol$^{-1}$) are marked in green, and variants with $\Delta\Delta G \geq -3.0$ kJ mol$^{-1}$ are marked in darker green. $K_i$ values were calculated as described in Materials and Methods. $K_i$ values were averaged, and mean value and standard deviation are shown. Relative $K_i$ values smaller than 0.7 are marked in green indicating variants with improved IL-5 inhibition compared to wild-type AF17121, and relative $K_i$ values ≥1.5 are in red indicating a decreased IL-5 inhibition. Mean values and standard deviation for absolute $K_D$ values are provided in Table S4.

tip of the β-turn we assumed that amino acid types modulating backbone flexibility and conformation might positively affect binding. In contrast to our assumption, replacement of Ser10 with either glycine or proline strongly decreased IL-5Rα binding; for example, S10G exhibited a 5- and S10P a more than 30-fold drop in binding affinity, respectively (Table 3). Hence, neither rigidifying nor relaxing the β-turn in AF17121 did benefit IL-5Rα–peptide binding. Surprisingly, however, mutation of Ser10 to alanine showed a 3- (25 °C) to 5-fold (37 °C) increased affinity. At 37 °C AF17121 S10A bound IL-5Rα with a $K_D$ of 8.8 ± 1.6 nM (Table 3), only 6.4-fold weaker than IL-5 bound to IL-5Rα ($K_D$ = 1.4 ± 0.02 nM determined using SPR at 35 °C). This unexpected affinity gain of AF17121 S10A likely is due to removal of unfavorable van der Waals contacts of the serine hydroxyl group with the aromatic ring of Trp190 located just beneath Ser10.

To test whether peptide-mediated inhibition of IL-5 signaling correlates with altered receptor binding, we established a bioassay measuring AF17121-mediated inhibition of IL-5-induced proliferation of erythroleukemic TF1 cells (Fig. 6A, B and Table 3). Twelve variants were tested. TF1 cells were stimulated with 200 pM IL-5 and wild-type AF17121 peptide or variants thereof were added in a concentration series (Table 3). As changes in affinity were rather small, measurement of half-maximal inhibitory concentrations ($IC_{50}$) might not be conclusive as small variations in experimental conditions could lead to statistically non-significant differences. Hence, for each experiment, the half-maximal effective concentration ($EC_{50}$) of IL-5 was

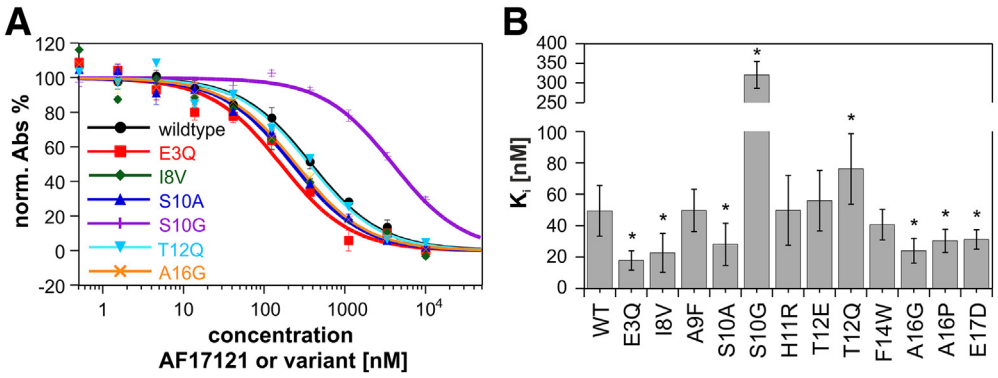


**Fig. 6.** IL-5 inhibition of AF17121 variants in IL-5-mediated TF-1 cell proliferation. (A) Dose-dependent inhibition of IL-5-induced TF-1 cell proliferation is shown for a selection of AF17121 variants; data were acquired in triplicate, normalized and fitted using the equation for determining $IC_{50}$ values and employing a Hill coefficient of 1. (B) The inhibitory constants $K_i$ were determined for AF17121 and 12 variants thereof (see Table 3). The $IC_{50}$ determined in triplicate in two fully independent measurements were transformed into six individual inhibitory constant ($K_i$) values, of which the mean value and standard deviation are shown as bar diagram. Statistical significance of the difference between the $K_i$ of wild-type AF17121 and that of the variants was determined by performing a Student *t* test assuming equal variances. *P*-values $\leq 0.05$ are marked with asterisk.

independently determined on the same microtiter plate. From these data, the inhibitory constants $K_i$ were determined, which allowed for better comparison of the IL-5 inhibition capacity of the AF17121 variants (Fig. 6B). Of the variants tested, A9F, T12E and F14W had inhibitory constants identical to wild-type AF17121 (Table 3). Variants H11R and T12Q exhibited slightly elevated $K_i$ values (1.3- and 1.4-fold), consistent with the reduced affinities of both peptide variants for IL-5Rα. The variant AF17121 S10G, which has a ~13-fold decreased binding for IL-5Rα at 37 °C, served as a control yielding a $K_i$ of 312 ± 28 nM, 6.5-fold greater than wild-type AF17121. Interestingly, besides AF17121 S10A, which had a 5-fold increased affinity for IL-5Rα, five other peptide variants showed a slightly improved inhibition of IL-5 signaling. While for S10A (relative $K_i$ 0.6), this was expected from *in vitro* binding data, the improved IL-5 inhibition by the variants E3Q (rel. $K_i$ 0.4), I8V (rel. $K_i$ 0.5), A16G (rel. $K_i$ 0.5), A16P (rel. $K_i$ 0.6) and E17D (rel. $K_i$ 0.7) is not backed by a corresponding affinity increase in IL-5Rα binding analyses. However, given the small improvements, which are 2-fold or less, and the comparably large variations of the $IC_{50}$ values observed in the individual measurements, data interpretation should be done with care. It seems therefore reasonable in upcoming studies to test whether the combination of several of these "efficacy-enhancing" mutations into one multivariant peptide leads to a statistically more significant improved IL-5 inhibition.

## Discussion

The role of IL-5 in eosinophil life and the significance of this type of granulocytes in the onset and progression of diseases commonly termed eosinophilia have drawn great interest in IL-5 signaling in pharmaceutical research [7,22]. This is highlighted by the numerous approaches to interfere with IL-5 signaling established over the past decade. Neutralizing antibodies have been developed against all components involved in IL-5 receptor activation: the ligand IL-5 (mepolizumab and reslizumab, [11,23]) as well as the receptors IL-5Rα (benralizumab, [24]) and βc (CSL311, [25]). Their effectiveness in abrogating IL-5 signaling, which decreases eosinophil count and relieves from disease symptoms, has led to FDA/EMA approval of mepolizumab (2015), reslizumab (2016) and benralizumab (2017) for therapy of severe eosinophilic asthma (see also Ref. [7]). IL-5 antagonists based on either the soluble IL-5Rα ectodomain or a variant of IL-5 have also been reported [26,27]. The inhibitors described so far all share the same disadvantages, that is, complex and costly production, targeting potentially limited by its size, possible immunogenic activity upon long-term application. However, a series of peptides, which have been discovered by library screening, abolish IL-5 signaling by blocking IL-5Rα and thereby present an alternative approach [13]. Two sorts of IL-5 inhibitory peptides were identified, one comprising monomeric disulfide-cyclized peptides and a second comprising almost twice as large, (homo-)dimeric disulfide-linked peptides. While the latter exhibit greater affinity for IL-5Rα and inhibit IL-5 signaling with higher efficacy, we focused on the monomeric peptides. Their smaller size (18mer *versus* 30mer) and their less complex inhibition mechanism through a 1:1 IL-5 competing interaction with IL-5Rα (dimeric peptides bind two IL-5Rα molecules) make them a better starting pharmacophore for subsequent optimization processes or small-molecule inhibitor design.

In this study, we have determined the structure of the peptide–receptor complex of the 18mer peptide AF17121 bound to the ectodomain of human IL-5Rα accompanied by an in-depth functional analysis that allowed to deduce principles of recognition and binding of AF17121 to IL-5Rα. We found that an intermolecular salt bridge between AF17121 Arg6 and the IL-5Rα Asp55 is the key interaction element of the peptide–receptor binding. Although this polar interaction resembles a similar motif in the IL-5–IL-5Rα interface, various differences between the peptide–IL-5Rα and the IL-5–IL-5Rα interfaces exist. While these data are of great interest for the development of peptide- or small molecule-based inhibitors of IL-5 signaling that can possibly be used in therapeutic applications targeting eosinophil-mediated diseases, the underlying structure–function relationship of the AF17121•IL-5Rα interaction might also provide general principles to design peptide mimetics targeting other cytokine receptors. So far, only very few examples of peptide mimetics targeting cell surface receptors have been described (e.g., see Ref. [28] and references therein) and only in case of the erythropoietin receptor-binding peptide mimetic EMP1 in-depth structure–function studies have been conducted [29–34]. While some features of the two peptide mimetics seem highly similar, that is, a small, less than 20mer peptide, which is cyclized through a single intramolecular disulfide (Fig. 7A), that shares no sequence similarity with the native ligand and directly binds to the respective receptor ectodomain with high specificity, a more detailed comparison shows that the IL-5 mimetic AF17121 and the erythropoietin (EPO) mimetic EMP1 share little commonalities. This is partly due to the different receptor activation mechanism found

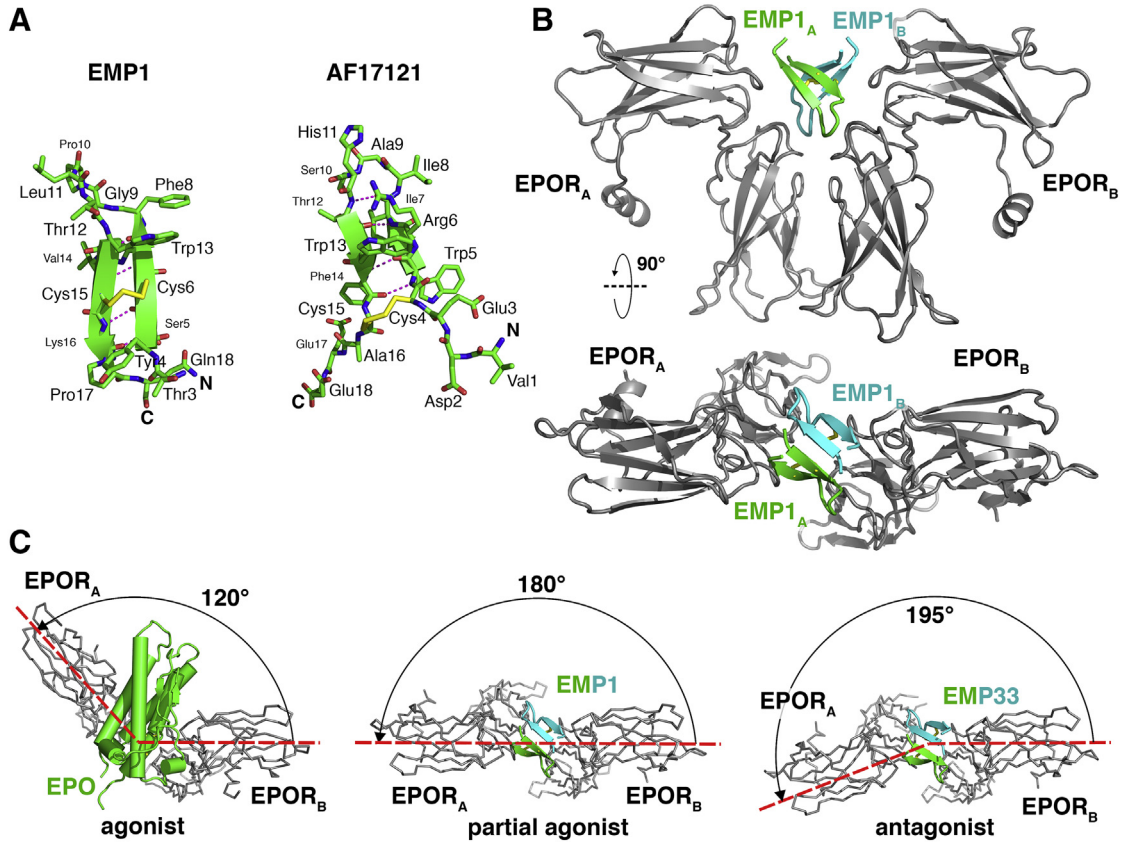


**Fig. 7.** Receptor binding and inhibition by AF17121 and the EPO mimetic EMP1 differ. (A) The EPO mimetic EMP1 (left) and the IL-5 mimetic AF17121 (right) have similar length and share a common β-hairpin loop architecture that is stabilized by an intramolecular disulfide bond. (B) Despite these similarities, EMP1 forms a non-covalent dimer (colored in green and cyan) and by binding one EPO receptor molecule to each monomer the dimeric peptide assembles two EPOR into a symmetrical heterotetrameric complex. (C) Modulating EPO receptor activation is more complex than in case of the IL-5 receptor. The native ligand EPO (left panel) assembles two EPO receptor molecules in an asymmetric complex in which both EPOR moieties arrange in an 120° orientation. In contrast, the partial agonist EMP1 (EMP1 does not activate EPO signaling to the same extent as EPO) yields a symmetrical assembly with both EPOR sharing a 180° arrangement. The EPO antagonist EMP33 (right panel) also binds two EPOR molecules due to its homodimeric nature but the two EPOR moieties arrange in a 195° arrangement, which is incompatible with EPO signaling.

for IL-5 and EPO. For IL-5 signaling a heteromeric receptor has to be assembled comprising IL-5Rα and βc, while a homodimeric receptor comprising two EPOR moieties is formed by EPO. Hence, a peptide such as AF17121 that binds to IL-5Rα but is incapable to recruit βc into a ternary complex inevitably acts as antagonist of IL-5. This holds still true for dimeric IL-5 peptide mimetics such as AF20016, which were shown to be efficient IL-5 antagonist by assembling two IL-5Rα molecules into a binary peptide–receptor complex [13]. In contrast, a symmetrical or dimeric peptide harboring both receptor binding sites of EPO could potentially recruit two EPO receptor moieties into a similar arrangement as the native ligand and might thereby act as EPO-like agonist. Structure analysis of an EMP1–EPOR complex revealed that EMP1 indeed functions a non-covalent dimer, which assembles two EPOR molecules into a complex and indeed exhibits EPO activity albeit with much lower efficacy (Fig. 7B) [29,30]. Structure analyses of EMP1•$(EPOR)_2$, EPO•$(EPOR)_2$ and a complex of an antagonistic EMP1 variant, EMP33•$(EPOR)_2$ then showed that EPOR signaling activity critically depends on the orientation of the two EPOR moieties in the complex [29,32,35]. Whereas the native ligand EPO assembles the two EPOR moieties in a 120° arrangement, EMP1, which has EPO activity, formed an EPOR assembly with perfect 2-fold symmetry arranging the two EPOR molecules at 180° (Fig. 7C). Interestingly, the EPO antagonist EMP33, which derives from EMP1 but carries an unnatural amino acid at position 4, still dimerizes two EPOR molecules as EMP1 but arranges the two EPOR moieties with a further 15° rotation beyond the 180° assembly initiated by EMP1 (Fig. 7C) [32]. Hence, generation of an EPO peptide mimetic with defined activity profile seems more complex than an IL-5 peptide-based antagonist.

Besides this different assembly mechanism, the two peptide mimetics AF17121 and EMP1 also on a molecular level bind their receptors quite differently. While neither AF17121 nor EMP1 exhibits any apparent sequence or structure homology with IL-5 and EPO, our structure analyses revealed that AF17121 and IL-5 similarly utilize an arginine, that is, Arg6 in AF17121 and Arg91 in IL-5, to form a high-energy salt bridge interaction with the same aspartate residue in IL-5Rα, that is, Asp55. Although the shielding of this intermolecular polar bond and its placement within the interface differs between AF17121 and IL-5, an analogous key interaction motif is found in both complexes, though. Thus, AF17121 indeed mimics a key interaction of the native ligand, although the much smaller size of the peptide (and hence the interface) requires adaptation of this intermolecular interaction to facilitate high-affinity binding. This is different when interfaces of EMP1•$(EPOR)_2$ and EPO•$(EPOR)_2$ are compared. Polar interactions dominate the binding of EPO to its receptors in both epitopes [35]. Syed *et al.* [35] list 17 h-bonds and salt bridges in the high-affinity binding site 1 and 11 polar bonds in the low-affinity site 2, while in EMP1•$(EPOR)_2$, only 6 h-bonds per epitope are found, none of them resembling any polar interaction found in EPO•$(EPOR)_2$ [29]. Instead hydrophobic interactions dominate the peptide–EPOR interface, and in particular, the interactions between the peptide's loop tip, which harbors an invariant key motif found in all selected EPO-mimicking peptides [30], and a loop of the second FNIII domain of EPOR have no comparable match in the EPO•$(EPOR)_2$ complex. This indicates that in contrast to the peptide-on-plasmid display selection of the antagonistic IL-5 mimetic AF17121, selection of EMP1 did not yield a peptide that directly (or even partly) mimics the EPO–EPOR interactions. Thus, AF17121 and EMP1 bind and modulate their respective receptor targets rather differently, indicating that similar size or a similar disulfide-linked cyclic loop architecture does not imply similar interaction mechanism or design principles.

With the detailed structure–function data of the AF17121•IL-5Rα interaction at hand, we attempted to find improved AF17121 analogs that exhibit higher affinities for IL-5Rα than the wild-type peptide and which would therefore possibly function as more effective IL-5 antagonists. From *in vitro* binding analyses, we identified variant AF17121 S10A, which showed a significantly increased affinity for IL-5Rα. Using cell-based assays to measure peptide-mediated attenuation of IL-5-induced cell proliferation, we found four additional amino acid exchanges that also possibly increase AF17121 antagonism. However, the effects of these single amino acid mutations were rather small and therefore claiming significant improvements seems not appropriate. Possibly combining all (or a subset) of these potentially improving mutations might yield an AF17121 multi-variant that exhibits a significantly increased affinity for IL-5Rα, which then translates into a more effective IL-5 antagonist.

In our approach, various amino acid replacements that were plausibly predicted *in silico* to improve peptide–receptor interaction, however, *in vitro* negatively affected receptor binding. This unexpected finding might be at the one hand due to our peptide design that utilized the crystal structure of the AF17121•IL-5Rα complex, which presents a static picture of the final bound state, but could not consider possible conformational rearrangements along the complex formation pathway. On the other hand, the design approach was further constrained by the limited chemical variability of proteinogenic amino acids, which presented the boundaries of our biosynthetic peptide production approach. To overcome both obstacles, upcoming studies should employ tailor-made structure-based peptide libraries

that utilize also non-natural amino acids for replacing individual residues of AF17121. Such an approach will certainly facilitate improving efficacy and other pharmacokinetic parameters to yield novel peptide-based IL-5 inhibitors for future therapies of eosinophil-mediated diseases.

## Materials and Methods

### Protein and peptide preparation

IL-5 and the ectodomain of IL-5Rα (comprising residues Asp21 to Arg335) and variants thereof were expressed in bacteria, refolded and purified as described [18]. All IL-5Rα ectodomain proteins harbor the mutation C66A, which replaces an unpaired cysteine located near the surface of the IL-5 receptor protein by alanine. This ensures increased protein stability and homogeneity as the free thiol group is prone to oxidation and modification by thiol-reactive reagents. Variants of IL-5Rα were generated by PCR applying the method by Weiner and Costa [36], mutations were verified by DNA sequencing. Purity and homogeneity of IL-5Rα proteins were analyzed by SDS-PAGE, analytical reversed-phase high-performance liquid chromatography and mass spectrometry. For MST-based interaction analyses, an IL-5Rα variant (ybbr–IL-5Rα) harboring an N-terminal 15mer amino acid extension containing the so-called ybbr sequence motif (-DSLEFIASKLA-; see below) was prepared similar to that described above.

For mutational analysis of AF17121, the peptide (amino acid sequence: VDECWRIIASHTWFCAEE) was expressed as cysteine protease-fusion protein. The cDNA encoding AF17121 was obtained by gene synthesis and comprised a NdeI site at the 5′ end in frame with the peptide sequence and a C-terminal LGS motif that contains a Leu required for proteolysis and a BamHI restriction site encoding for Gly–Ser needed for ligation. The DNA was cloned between the NdeI and BamHI restriction sites of a modified pET22 expression vector (pET22b-CPD-$_{BamHI\text{-}Leu}$) that contained the *Vibrio cholerae* MARTX toxin cysteine protease domain and a C-terminal sequence encoding hexahistidine at the 3′ end of the BamHI site [21]. Transformed BL21(DE3)Star cells were grown in Terrific Broth medium at 37 °C, for protein expression the culture was cooled down to 18 °C and supplemented with 1 mM IPTG. Protein expression proceeded for 12 h; thereafter, cells were harvested by centrifugation (6000*g*, 4 °C, 25 min), resuspended in 50 mM Tris–HCl (pH 7.5) and 500 mM NaCl, and lysed by sonication. Cell lysates were cleared by centrifugation (33,800*g*, 4 °C, 45 min) and the supernatant was incubated for 12 h at 4 °C. The lysate was subjected to immobilized metal ion affinity chromatography employing a HisTrap excel column (GE Healthcare). AF17121–cysteine protease domain fusion protein was eluted with 500 mM imidazole, pooled and dialyzed against 50 mM Tris–HCl (pH 7.5) and 500 mM NaCl. The fusion protein was concentrated to ≥2.4 mM by ultrafiltration, and intramolecular proteolysis by the MARTX toxin cysteine protease domain was induced by addition of myo-inositol hexakisphosphate to a concentration of 1 mM. The mixture was incubated at 37 °C for 1 h, after which the solution was kept at 4 °C. Possible precipitate was removed by centrifugation (16,800*g*, 4 °C, 25 min), and the clear supernatant was subjected to gel filtration employing a Superdex peptide HR 10/30 column (GE Healthcare) and using 10 mM Hepes (pH 7.4), 150 mM NaCl and 3.4 mM EDTA as running buffer. AF17121-containing fractions were pooled, concentrated by ultrafiltration and stored at −20 °C until further use. Peptide purity and homogeneity were analyzed by SDS-PAGE, reversed-phase high-performance liquid chromatography and mass spectrometry. Variants of AF17121 were generated by PCR employing the method of Weiner and Costa [36], and mutations were verified by DNA sequencing.

### Crystallization and structure determination of the AF17121•IL-5Rα complex

For structure determination of the peptide–IL-5Rα complex, AF17121 was obtained by chemical synthesis with a purity greater than 90% (Centic Biotec). The complex was prepared by mixing IL-5Rα C66A ectodomain protein and AF17121 in a 1:1.2 molar ratio and subsequently purifying the peptide–protein complex by gel filtration employing a Superdex 200 10/300 column (GE Healthcare) and using 10 mM Hepes (pH 7.4), 150 mM NaCl and 3.4 mM EDTA ($HBSE_{150}$) as running buffer. Complex-containing fractions were pooled and concentrated to 7 mg/ml. Crystals were grown by sitting-drop vapor diffusion from 0.1 M sodium acetate pH 5.0, 3% (w/v) polyethylene glycol 4000, 15% or 20% (v/v) 2-methyl-2,4-pentanediol using a protein/precipitant ratio of 1:1 in the droplet within 14 days. For diffraction data acquisition, crystals were directly flash-cooled in liquid nitrogen. A high-resolution data set with a maximal resolution of 2.75 Å was obtained from the beamline MX1-P13 at PETRA III at the synchrotron facility DESY (Hamburg). Data were processed using iMOSFLM, AIMLESS and SCALA of the CCP4 program suite version 7.0 [37,38].

The structure of AF17121•IL-5Rα was determined by molecular replacement employing the software PHASER from the CCP4 program suite and the coordinates of the ectodomain of IL-5Rα from the PDB dataset 3QT2 [18,39]. As it was unknown as to whether the architectures of the IL-5Rα ectodomain

bound to IL-5 and bound to AF17121 are identical, a first PHASER search testing both possible enantiomeric space groups $P6_222$ and $P6_422$ was conducted with the IL-5Rα template structure dissected into its three fibronectin type III subdomains D1 (7–102), D2 (103–220) and D3 (221–313). An unambiguous solution was obtained identifying the correct space group $P6_422$ with the three subdomains arranged in the identical wrench-like architecture as in the initial IL-5Rα template derived from the coordinate set 3QT2. To confirm this finding, two further PHASER MR searches were performed, the first employing two search templates comprising the CRM/D2D3 motif (108–313) and the individual subdomain D1 (7–102) and a second run employing the complete IL-5Rα ectodomain (7–313) in its conformation bound to IL-5 as search template. Using the results from the PHASER molecular replacement runs, initial difference electron density maps were calculated, which allowed for unambiguous modeling of residues Val1 to Glu18 of the cyclic peptide AF17121 into the electron density map. The structure of the complex of AF17121•IL-5Rα was then solved by iterative cycles of refinement using the software PHENIX (version 1.9–1692) and manual model building using the software Quanta2008 (MSI Accelrys) and Coot (version 0.8.9.1) [40,41]. Data collection and refinement statistics are outlined in Table 1. Figures showing structural models and electron density were prepared with the software Pymol (Schroedinger).

## SPR

Biosensor-based interaction analyses were performed using a ProteOn XPR36 system (Biorad). All measurements were done at 25 °C and a flowrate of 100 µl $min^{-1}$ and employing 10 mM Hepes (pH 7.4), 150 mM NaCl, 3.4 mM EDTA and 0.005% (v/v) Tween20 ($HBST_{150}$) unless stated otherwise. IL-5 was biotinylated with a 2-fold molar excess (protein: biotin) of EZ-Link™ Sulfo-NHS-Biotin (Thermo Fisher) according to the manufacturer's recommendation, and non-reacted biotin was removed by size exclusion chromatography using PD10 columns (GE Healthcare). Biotinylated AF17121 peptide, which carries a biotin moiety attached to the N-terminus of a Gly–Ser spacer, was obtained with a purity greater than 90% by chemical synthesis from Centic Biotec. For immobilization, a GLC sensor chip (Bio-Rad) was first activated with *N*-hydroxysulfosuccinimide (Sulfo-NHS) and *N*-(3-dimethylaminopropyl)-*N*-ethylcarbodiimide (EDC; Biorad) according to the manufacturer's recommendation. Neutravidin (Sigma-Aldrich) dissolved in 10 mM sodium acetate (pH 4.5) was perfused over the activated sensor matrix at a concentration of 40 µg $ml^{-1}$ until resonance unit (RU) levels reached about 3500 RU (1 RU = 1 pg $mm^{-2}$). Biotinylated IL-5 and AF17121 were then captured onto the neutravidin-coated sensor surface at densities of about 200 to 250 RU (for IL-5) and about 100 to 150 RU (for AF17121). For SPR data acquisition, IL-5Rα proteins were perfused as analytes over the biosensor employing six concentrations typically ranging from 250 to 7.8 nM for binding data of AF17121 and from 15.6 to 0.5 nM for acquisition of IL-5 binding data and typically observing association for 200 s (association time). Dissociation was monitored by perfusing $HBST_{150}$ buffer for typically 120 s. Biosensor regeneration was performed by injecting 10 mM glycine (pH 2.5) for 30s. The association and dissociation phases of the sensogram were fitted with a Langmuir-type 1:1 interaction model with all fitting parameters usually evaluated group wise using the software ProteOn Manager version 3.1 (Biorad). Data were only interpreted if $\chi^2$ values were less than 10% of the maximal signal amplitude ($RU_{max}$). Equilibrium binding constants $K_D$ were calculated from the equation $K_D = k_{off}/k_{on}$. All affinities are termed "apparent" $K_D$ values, indicating that the absolute values might differ from values obtained by other interaction analysis methods. Differences in affinities and rate constants determined in this study greater than 2-fold were considered significant.

## MST

Interaction analyses in solution were performed using MST employing a Monolith NT.115 device (NanoTemper). YbbR–IL-5Rα protein was site-specifically labeled with the Dyomics dye DY-647P1 employing enzymatic coupling of the CoA-647 substrate, a CoA-DY-647P1 conjugate, by Sfp phosphopantetheinyl transferase (New England Biolabs) [42,43]. The fluorescent dye is hereby covalently attached to the first serine residue in the ybbR sequence (-DSLEFIASKLA-). Labeling was performed by mixing purified ybbR–IL-5Rα protein and CoA-647 in a 1:1.5 molar ratio and incubating the mixture in the presence of 0.5 µM Sfp synthase (New England Biolabs) for 2 h at 22 °C in the dark. Non-reacted CoA-647 substrate was removed by size exclusion chromatography employing a Superdex 200 Increase 10/300 GL column (GE Healthcare). Labeling efficiency for ybbR–IL-5Rα was found to be about 50% as determined from measuring absorbance at 280 and 650 nm. For thermophoresis experiments, serial dilution series of the different AF17121 variants ranging from 20 µM to 0.6 nM in the presence of 29 nM labeled IL-5Rα were prepared using 10 mM Hepes (pH 8.0), 150 mM NaCl, 3.4 mM EDTA and 0.05% (v/v) Tween20 as buffer. Samples were incubated for 5 min at room temperature, centrifuged at 16,000*g*, 4 °C for 30 min and loaded into standard capillaries (NanoTemper). For MST measurements at 25 °C, thermophoresis temperature gradient was 60% infrared (IR) laser power and LED power for fluorescence excitation was 60%; for measurements at 37 °C,

IR laser power was at 60% and fluorescence excitation was 70% LED laser power. Data were obtained from two independent measurement series with each acquisition done in triplicate. Data analyses were performed using the software NanoTemper Analysis version 2.1.2333. Binding affinities are mean values with standard deviation derived from six binding experiments. As for SPR data, affinities are termed apparent affinities to indicate that the values obtained with MST might differ from binding data derived from other *in vitro* interaction analysis methods. Again, differences greater than 2-fold were considered significant.

### TF1 cell proliferation-based peptide competition assay

IL-5 activity was determined from dose-dependent IL-5-mediated cell viability measured by enzymatic conversion of resazurin. As human erythroleukemic TF1 cells do usually not respond to IL-5, IL-5-responsive cells were selected by cultivating TF1 cells in GM-CSF-depleted medium containing IL-5 following published protocols (see Fig. S5) [44]. Such selected cells were cultured in RPMI 1640 + GlutaMAX™-I medium (Thermo Fischer) supplemented with 1% (v/v) penicillin–streptomycin solution (Lonza) and 10% (v/v) heat-inactivated fetal calf serum (Biochrome) and 5 ng/ml hIL-5. For the assay, cells were washed with factor-free medium, seeded in microtiter plates with 96 flat-bottomed wells at a density of $3 \times 10^5$ cells per well and incubated at 37 °C, 5% $CO_2$ in the presence of 200 pM IL-5. Inhibition of IL-5 activity through competition was determined by supplementing the wells with increasing concentrations of AF17121 or variants thereof (from 10 μM to 0.5 nM). After incubation for 72 h, 10 μl of resazurin solution in PBS (concentration 0.15 mg $ml^{-1}$) was added to each well and the mixture was incubated at 37 °C for 4 h. Relative cell numbers were determined by measuring the absorbance at 571 nm and subtracting the background at 749 nm. Values were obtained from performing two fully independent measurement series in which IL-5 inhibition of each peptide was determined as triplicate from a single plate. Absorbance values were normalized to 0% for background absorbance and 100% for absorbance values of IL-5-stimulated cells without peptide. $IC_{50}$ values were obtained by fitting each experiment applying the $IC_{50}$ fitting routine from the software KaleidaGraph version 4.5 (Synergy) using a Hill coefficient of 1. On each plate, also the $EC_{50}$ of IL-5 was determined in duplicate. From $IC_{50}$ (IL-5 competition by AF17121 or a variant thereof) and $EC_{50}$ (IL-5) values (Fig. S5), the inhibitory constant of the respective peptide was calculated from the equation $K_i = IC_{50}/(([IL\text{-}5]_{stimulatory}/EC_{50}) + 1)$, with $IC_{50}$ being the $IC_{50}$ value of the respective AF17121 peptide, $[IL5]_{stimulatory}$ being the fixed concentration of IL-5 used in the competition series (i.e., 200 pM) and $EC_{50}$ being the half-maximal effective concentration of IL-5 determined on the same microtiter plate as the peptide/peptide variant. The statistical significance of the difference between the $K_i$ of wild-type AF17121 and that of variants of AF17121 investigated was determined by performing a Student *t* test assuming equal variances in KaleidaGraph version 4.5.

### Accession numbers

Coordinates and structure factors of the AF17121•IL-5Rα complex have been deposited in the Protein Data Bank databank (www.rcsb.org) under accession code 6H41.

## CRediT authorship contribution statement

**Jan-Philipp Scheide-Noeth:** Methodology, Investigation, Writing - original draft, Writing - review & editing, Resources. **Maximilian Rosen:** Investigation. **David Baumstark:** Investigation.
**Harald Dietz:** Investigation. **Thomas D. Mueller:** Conceptualization, Methodology, Investigation, Data curation, Writing - original draft, Writing - review & editing, Funding acquisition, Resources, Project administration, Supervision.

## Acknowledgments

The authors thank Eva Wirth and Eva-Maria Muth for excellent technical assistance and Werner Schmitz (Department of Molecular Biology and Biochemistry, Biocenter University Wuerzburg) for mass spectrometry analyses. We acknowledge access to the X-ray facility at the Rudolf-Virchow Center of the University Wuerzburg and to the synchrotron beamline Petra III MX1-P13 at DESY, Hamburg. This project was supported by Deutsche Forschungsgemeinschaft grant MU1095/7-1.

**Declaration of Interests:** The authors declare that they have no conflict of interest.

## Appendix A. Supplementary data

Supplementary data to this article can be found online at https://doi.org/10.1016/j.jmb.2018.11.029.

*Received 16 October 2018;*
*Received in revised form 21 November 2018;*
*Accepted 28 November 2018*
Available online 7 December 2018

***Keywords:***
atopic diseases;
eosinophil;
interleukin-5 signaling;
peptide-based interleukin-5 inhibitor;
peptide engineering

***Abbreviations used:***
IL, interleukin; SPR, surface plasmon resonance; RU, resonance unit; MST, microscale thermophoresis.

## References

[1] A.D. Klion, T.B. Nutman, The role of eosinophils in host defense against helminth parasites, J. Allergy Clin. Immunol. 113 (2004) 30–37.
[2] P.F. Weller, E.J. Goetzl, The human eosinophil: roles in host defense and tissue injury, Am. J. Pathol. 100 (1980) 791–820.
[3] W. Liao, H. Long, C.C. Chang, Q. Lu, The eosinophil in health and disease: from bench to bedside and back, Clin. Rev. Allergy Immunol. 50 (2016) 125–139.
[4] H. Kita, Eosinophils: multifunctional and distinctive properties, Int. Arch. Allergy Immunol. 161 (Suppl. 2) (2013) 3–9.
[5] C. Curtis, P. Ogbogu, Hypereosinophilic syndrome, Clin. Rev. Allergy Immunol. 50 (2016) 240–251.
[6] T. Yanagibashi, M. Satoh, Y. Nagai, M. Koike, K. Takatsu, Allergic diseases: from bench to clinic—contribution of the discovery of interleukin-5, Cytokine 98 (2017) 59–70.
[7] F. Roufosse, Targeting the interleukin-5 pathway for treatment of eosinophilic conditions other than asthma, Front. Med. (Lausanne) 5 (2018) 49.
[8] T.R. Hercus, U. Dhagat, W.L. Kan, S.E. Broughton, T.L. Nero, M. Perugini, et al., Signalling by the betac family of cytokines, Cytokine Growth Factor Rev. 24 (2013) 189–201.
[9] T. Kitamura, N. Sato, K. Arai, A. Miyajima, Expression cloning of the human IL-3 receptor cDNA reveals a shared beta subunit for the human IL-3 and GM-CSF receptors, Cell 66 (1991) 1165–1174.
[10] J. Tavernier, R. Devos, S. Cornelis, T. Tuypens, J. Van der Heyden, W. Fiers, et al., A human high affinity interleukin-5 receptor (IL5R) is composed of an IL5-specific alpha chain and a beta chain shared with the receptor for GM-CSF, Cell 66 (1991) 1175–1184.
[11] T.K. Hart, R.M. Cook, P. Zia-Amirhosseini, E. Minthorn, T.S. Sellers, B.E. Maleeff, et al., Preclinical efficacy and safety of mepolizumab (SB-240563), a humanized monoclonal antibody to IL-5, in cynomolgus monkeys, J. Allergy Clin. Immunol. 108 (2001) 250–257.
[12] R. Kolbeck, A. Kozhich, M. Koike, L. Peng, C.K. Andersson, M.M. Damschroder, et al., MEDI-563, a humanized anti-IL-5 receptor alpha mAb with enhanced antibody-dependent cell-mediated cytotoxicity function, J. Allergy Clin. Immunol. 125 (2010) 1344–1353 (e2).
[13] B.P. England, P. Balasubramanian, I. Uings, S. Bethell, M.J. Chen, P.J. Schatz, et al., A potent dimeric peptide antagonist of interleukin-5 that binds two interleukin-5 receptor alpha chains, Proc. Natl. Acad. Sci. U. S. A. 97 (2000) 6862–6867.
[14] P. Ruchala, G. Varadi, T. Ishino, J. Scibek, M. Bhattacharya, C. Urbina, et al., Cyclic peptide interleukin 5 antagonists mimic CD turn recognition epitope for receptor alpha, Biopolymers 73 (2004) 556–568.
[15] T. Ishino, C. Urbina, M. Bhattacharya, D. Panarello, I. Chaiken, Receptor epitope usage by an interleukin-5 mimetic peptide, J. Biol. Chem. 280 (2005) 22951–22961.
[16] T. Ishino, U. Pillalamarri, D. Panarello, M. Bhattacharya, C. Urbina, S. Horvat, et al., Asymmetric usage of antagonist charged residues drives interleukin-5 receptor recruitment but is insufficient for receptor activation, Biochemistry 45 (2006) 1106–1115.
[17] M. Bhattacharya, U. Pillalamari, S. Sarkhel, T. Ishino, C. Urbina, B. Jameson, et al., Recruitment pharmacophore for interleukin 5 receptor alpha antagonism, Biopolymers 88 (2007) 83–93.
[18] E. Patino, A. Kotzsch, S. Saremba, J. Nickel, W. Schmitz, W. Sebald, et al., Structure analysis of the IL-5 ligand–receptor complex reveals a wrench-like architecture for IL-5Ralpha, Structure 19 (2011) 1864–1875.
[19] T. Ishino, A.E. Harrington, H. Gopi, I. Chaiken, Structure-based rationale for interleukin 5 receptor antagonism, Curr. Pharm. Des. 14 (2008) 1231–1239.
[20] S. Kusano, M. Kukimoto-Niino, N. Hino, N. Ohsawa, M. Ikutani, S. Takaki, et al., Structural basis of interleukin-5 dimer recognition by its alpha receptor, Protein Sci. 21 (2012) 850–864.
[21] A. Shen, P.J. Lupardus, M. Morell, E.L. Ponder, A.M. Sadaghiani, K.C. Garcia, et al., Simplified, enhanced protein purification using an inducible, autoprocessing enzyme tag, PLoS One 4 (2009), e8119. .
[22] C. Domingo, Overlapping effects of new monoclonal antibodies for severe asthma, Drugs 77 (2017) 1769–1787.
[23] J.C. Kips, B.J. O'Connor, S.J. Langley, A. Woodcock, H.A. Kerstjens, D.S. Postma, et al., Effect of SCH55700, a humanized anti-human interleukin-5 antibody, in severe persistent asthma: a pilot study, Am. J. Respir. Crit. Care Med. 167 (2003) 1655–1659.
[24] M. Koike, K. Nakamura, A. Furuya, A. Iida, H. Anazawa, K. Takatsu, et al., Establishment of humanized anti-interleukin-5 receptor alpha chain monoclonal antibodies having a potent neutralizing activity, Hum. Antibodies 18 (2009) 17–27.
[25] C. Panousis, U. Dhagat, K.M. Edwards, V. Rayzman, M.P. Hardy, H. Braley, et al., CSL311, a novel, potent, therapeutic monoclonal antibody for the treatment of diseases mediated by the common beta chain of the IL-3, GM-CSF and IL-5 receptors, MAbs 8 (2016) 436–453.
[26] J. Tavernier, T. Tuypens, A. Verhee, G. Plaetinck, R. Devos, J. Van der Heyden, et al., Identification of receptor-binding domains on human interleukin 5 and design of an interleukin 5-derived receptor antagonist, Proc. Natl. Acad. Sci. U. S. A. 92 (1995) 5194–5198.
[27] N. Tsuruoka, K. Yamashiro, M. Tsujimoto, Purification of soluble murine interleukin 5 (IL-5) receptor alpha expressed in Chinese hamster ovary cells and its action as an IL-5 antagonist, Arch. Biochem. Biophys. 307 (1993) 133–137.
[28] M. Atanasova, A. Whitty, Understanding cytokine and growth factor receptor activation mechanisms, Crit. Rev. Biochem. Mol. Biol. 47 (2012) 502–530.
[29] O. Livnah, E.A. Stura, D.L. Johnson, S.A. Middleton, L.S. Mulcahy, N.C. Wrighton, et al., Functional mimicry of a protein hormone by a peptide agonist: the EPO receptor complex at 2.8 a, Science 273 (1996) 464–471.
[30] N.C. Wrighton, F.X. Farrell, R. Chang, A.K. Kashyap, F.P. Barbone, L.S. Mulcahy, et al., Small peptides as potent mimetics of the protein hormone erythropoietin, Science 273 (1996) 458–464.
[31] D.L. Johnson, F.X. Farrell, F.P. Barbone, F.J. McMahon, J. Tullai, D. Kroon, et al., Amino-terminal dimerization of an

erythropoietin mimetic peptide results in increased erythropoietic activity, Chem. Biol. 4 (1997) 939–950.
[32] O. Livnah, D.L. Johnson, E.A. Stura, F.X. Farrell, F.P. Barbone, Y. You, et al., An antagonist peptide–EPO receptor complex suggests that receptor dimerization is not sufficient for activation, Nat. Struct. Biol. 5 (1998) 993–1004.
[33] S.A. Middleton, F.P. Barbone, D.L. Johnson, R.L. Thurmond, Y. You, F.J. McMahon, et al., Shared and unique determinants of the erythropoietin (EPO) receptor are important for binding EPO and EPO mimetic peptide, J. Biol. Chem. 274 (1999) 14163–14169.
[34] O. Vadas, O. Hartley, K. Rose, Characterization of new multimeric erythropoietin receptor agonists, Biopolymers 90 (2008) 496–502.
[35] R.S. Syed, S.W. Reid, C. Li, J.C. Cheetham, K.H. Aoki, B. Liu, et al., Efficiency of signalling through cytokine receptors depends critically on receptor orientation, Nature 395 (1998) 511–516.
[36] M.P. Weiner, G.L. Costa, Rapid PCR site-directed mutagenesis, PCR Methods Appl. 4 (1994) S131–S136.
[37] T.G. Battye, L. Kontogiannis, O. Johnson, H.R. Powell, A.G. Leslie, iMOSFLM: a new graphical interface for diffraction-image processing with MOSFLM, Acta Crystallogr. D Biol. Crystallogr. 67 (2011) 271–281.
[38] M.D. Winn, C.C. Ballard, K.D. Cowtan, E.J. Dodson, P. Emsley, P.R. Evans, et al., Overview of the CCP4 suite and current developments, Acta Crystallogr. D Biol. Crystallogr. 67 (2011) 235–242.
[39] A.J. McCoy, R.W. Grosse-Kunstleve, P.D. Adams, M.D. Winn, L.C. Storoni, R.J. Read, Phaser crystallographic software, J. Appl. Crystallogr. 40 (2007) 658–674.
[40] P.D. Adams, P.V. Afonine, G. Bunkoczi, V.B. Chen, I.W. Davis, N. Echols, et al., PHENIX: a comprehensive python-based system for macromolecular structure solution, Acta Crystallogr. D Biol. Crystallogr. 66 (2010) 213–221.
[41] P. Emsley, B. Lohkamp, W.G. Scott, K. Cowtan, Features and development of coot, Acta Crystallogr. D Biol. Crystallogr. 66 (2010) 486–501.
[42] J. Yin, A.J. Lin, D.E. Golan, C.T. Walsh, Site-specific protein labeling by Sfp phosphopantetheinyl transferase, Nat. Protoc. 1 (2006) 280–285.
[43] J. Yin, P.D. Straight, S.M. McLoughlin, Z. Zhou, A.J. Lin, D.E. Golan, et al., Genetically encoded short peptide tag for versatile protein labeling by Sfp phosphopantetheinyl transferase, Proc. Natl. Acad. Sci. U. S. A. 102 (2005) 15815–15820.
[44] J.J. Yen, Y.C. Hsieh, C.L. Yen, C.C. Chang, S. Lin, H.F. Yang-Yen, Restoring the apoptosis suppression response to IL-5 confers on erythroleukemic cells a phenotype of IL-5-dependent growth, J. Immunol. 154 (1995) 2144–2152.